

# Unraveling demographic patterns in tropical birds across an elevational gradient

Montague H. C. Neate-Clegg,<sup>1,2,\*</sup>  James F. Saracco,<sup>3</sup>  Fabiola Rodríguez-Vásquez,<sup>4</sup>  and Samuel E. I. Jones<sup>5,\*</sup> 

<sup>1</sup>Environmental Studies, University of California, Santa Cruz, California, USA

<sup>2</sup>Ecology and Evolutionary Biology, University of California, Los Angeles, California, USA

<sup>3</sup>The Institute for Bird Populations, Petaluma, California, USA

<sup>4</sup>Cornell Lab of Ornithology, Cornell University, Ithaca, New York, USA

<sup>5</sup>School of Biological Sciences, Georgia Institute of Technology, Atlanta, Georgia, USA

\*Corresponding authors: Montague H. C. Neate-Clegg, [monteneateclegg@gmail.com](mailto:monteneateclegg@gmail.com); Samuel E. I. Jones, [samuel.ei.jones@gmail.com](mailto:samuel.ei.jones@gmail.com)

## ABSTRACT

An increasing body of evidence has displayed upslope shifts in the high-diversity avian communities of tropical mountains. Such shifts have largely been attributed to warming climates, although their actual mechanisms remain poorly understood. One likely possibility is that changes in species-specific demographic rates underlie elevational range shifts. Fine-scale population monitoring and capture–mark–recapture (CMR) analysis could shed light on these mechanisms, but, until recently, analytical constraints have limited our ability to model multiple demographic rates across bird communities while accounting for transient individuals. Here, we used Bayesian hierarchical multi-species CMR models to estimate the apparent survival, recruitment, and realized population growth rates of 17 bird species along an elevational gradient in the cloud forests of Honduras. For 6 species, we also modeled demographic rates across elevation and time. Although demographic rates varied among species, population growth rates tended to be higher in lower elevation species. Moreover, some species showed higher population growth rates at higher elevations, and elevational differences in growth rates were positively associated with previous estimates of upslope shifts at the study site. We also found that demographic rates showed contrasting trends across the duration of the study, with recruitment decreasing and apparent survival increasing, and stronger effects at lower elevations. Collectively, we provide the methodological tools to encourage more multi-species demographic analyses in other systems, while highlighting the potential for the demographic impacts of global change. We provide a Spanish translation in the [Supplementary Materials](#).

**Keywords:** apparent survival, climate change, cloud forest, capture–mark–recapture models, escalator to extinction, Mesoamerica, realized population growth rate, recruitment rate

## How to Cite

Neate-Clegg, M. H. C., J. F. Saracco, F. Rodríguez-Vásquez, and S. E. I. Jones (2024). Unraveling demographic patterns in tropical birds across an elevational gradient. *Ornithological Applications* 127:duae063.

## LAY SUMMARY

- Climate change is causing tropical birds to shift to higher elevations but little is known about the population mechanisms underpinning these shifts.
- Until now, studies along tropical mountain ranges have been limited by a lack of long-term monitoring data as well as inadequate modeling techniques.
- We use Bayesian hierarchical mark–recapture models to estimate avian population parameters across an elevational gradient in Honduras from a 12-year constant effort banding project.
- We report baseline population parameters for 17 species, and show variation in those parameters across elevation and time for 6 species, supporting previous evidence of upslope shifts at the site.
- Using this analytical framework, we encourage others to analyze population parameters in tropical birds to increase our global picture of life history, and of anthropogenic impacts on demography.

Descifrando los patrones demográficos de las aves tropicales a través de un gradiente de elevación

## RESUMEN

Cada vez hay más pruebas de que las comunidades de aves de alta diversidad en las montañas tropicales han mostrado desplazamientos a zonas de mayor elevación. Estos desplazamientos se han atribuido en gran medida al calentamiento del clima, aunque sus mecanismos siguen siendo poco conocidos. Una posibilidad es que los cambios en las tasas demográficas específicas de cada especie subyazcan a los desplazamientos altitudinales. El monitoreo de poblaciones a pequeña escala y los análisis de captura-marcaje-recaptura (CMR) podrían esclarecer estos mecanismos pero las restricciones analíticas han limitado nuestra capacidad para modelar tasas demográficas múltiples en las comunidades de aves teniendo en cuenta a los individuos transitorios. En esta investigación, utilizamos modelos CMR, jerárquicos, para múltiples especies, en un marco bayesiano para estimar la supervivencia aparente, el reclutamiento y las tasas de crecimiento poblacional realizadas de 17 especies de aves en un gradiente altitudinal en un bosque nuboso de Honduras. Para seis especies, también modelamos las tasas demográficas a través de la elevación y el tiempo. Aunque las tasas demográficas variaron entre especies, las tasas de crecimiento poblacional a mayores elevaciones, y estas diferencias altitudinales en las tasas de crecimiento se asociaron positivamente con estimaciones previas de desplazamientos a zonas de mayor elevación en la misma área de estudio. También observamos que estas tasas mostraron tendencias opuestas durante el estudio, con una disminución del reclutamiento y un aumento de la supervivencia aparente, siendo estos efectos más fuertes a menor elevación. En conjunto, proporcionamos herramientas metodológicas para fomentar más análisis demográficos multi-especie en otros sistemas y destacamos el potencial de los impactos demográficos del cambio global.

**Palabras clave:** bosque nuboso, cambio climático, escalera a la extinción, Mesoamérica, modelos de captura-marcaje-recaptura, supervivencia aparente, tasa de crecimiento poblacional realizado, tasa de reclutamiento

## INTRODUCTION

Elevational gradients in the tropics are global centers of biodiversity, rich in endemism and species turnover (Myers et al. 2000, Quintero and Jetz 2018, Rahbek et al. 2019, Jarzyna et al. 2021). Global warming is one of the greatest threats to tropical montane ecosystems (Williams and Jackson 2007, Şekercioğlu et al. 2012) and has been implicated in upslope shifts in montane birds across tropical and temperate systems alike (Lenoir et al. 2020, Freeman et al. 2021, Neate-Clegg and Tingley 2023). The consensus view of elevational shifts has been “niche tracking,” whereby a species tracks its thermal niche upslope. However, substantial variation in shift rates across species and locations (Lenoir et al. 2020, Neate-Clegg et al. 2021a) suggests that temperature tracking alone is not sufficient to explain range shifts. Beyond temperature, other abiotic factors (e.g., precipitation) and biotic interactions (e.g., habitat availability, competition, and natural enemies) could shape elevational redistributions (Jankowski et al. 2012, Tingley et al. 2012, Neate-Clegg and Tingley 2023).

A pervasive challenge affecting our ability to understand the mechanisms that underlie range shifts in tropical mountains (Beissinger and Riddell 2021, Neate-Clegg and Tingley 2023) is a lack of long-term monitoring studies (but see: Neate-Clegg et al. 2020, Williams and De la Fuente 2021, Briscoe et al. 2021). Few tropical sites are monitored for long enough to provide the requisite survey data needed to make population-level inferences about elevational shifts (Forero-Medina et al. 2011, Freeman and Class Freeman 2014, Neate-Clegg et al. 2021c) and temporal variability in distributions (Neate-Clegg et al. 2020, Maicher et al. 2020). Evidence for range shifts has thus been largely derived from estimates based on annual point count data (Neate-Clegg et al. 2018, 2020) or multi-decade resurveys (Forero-Medina et al. 2011, Freeman and Class Freeman 2014, Freeman et al. 2018). Yet, elevational shifts are likely fundamentally underpinned by demographic processes, and an alternative approach to understanding these range shifts is through examining demographic parameters across elevation, estimated from capture–mark–recapture (CMR) models (Srinivasan and Wilcove 2021).

Among the options for CMR modeling, “reverse-symmetry” CMR models (Pradel 1996) are especially attractive, as they exploit information in both the forward and backward directions of capture histories to inform survival and recruitment parameters, as well as population growth rates, providing in-

ferences about the causes of population change. For a species shifting its elevational range upslope, we might expect such models to evidence population increases at the leading edge of the elevational range, and population declines at the trailing edge. In this instance, population growth rates at the leading edge could plausibly be driven by increases in recruitment rates, while population declines at the trailing edge could be driven by decreasing survival rates. A growing number of bird-banding datasets in the tropics (Wolfe et al. 2015, Ryder and Sillett 2016, Brawn et al. 2017, Srinivasan and Wilcove 2021) now surpass 10 years of data, the typical threshold for simple CMR models (Ruiz-Gutiérrez et al. 2012). Besides revealing trends over time, such datasets and CMR models are also invaluable for estimating baseline demographic rates of birds (Ruiz-Gutiérrez et al. 2012, Kittelberger et al. 2021), which remain poorly known across tropical birds (Sheldon 2019).

A particular analytical challenge with these data is that tropical forest birds are generally characterized by low capture rates, which has traditionally limited demographic inference to just a few of the most commonly captured species (Ruiz-Gutiérrez et al. 2012). One solution to obtaining estimates for more species (improving our ability to interrogate the demographic mechanisms underlying range shifts) is to implement hierarchical multi-species models that assume that at least some species-specific model parameters are drawn from a common distribution (i.e., “species as random effects”). This model flexibility is not available for popular frequentist-based CMR software programs, such as MARK (Cooch and White 2006, Laake and Rexstad 2006), but can be implemented in a Bayesian context (Kéry and Schaub 2011, Tenan et al. 2014, Saracco et al. 2022). However, one common feature of bird populations that can complicate inferences from CMR models is the presence of transient individuals (i.e., individuals that are just passing through that do not contribute to the local population demographics). Not accounting for these individuals can result in underestimation of apparent survival (Pradel et al. 1997). Until recently, reverse-symmetry models have not been able to account for transient individuals, limiting the utility of these models for many applications. Telenský et al. (2023) outlined a formulation of the reverse-symmetry CMR model in a Bayesian framework that addresses this limitation; the flexibility of this modeling framework—including residency, population growth rate, recruitment rate, and apparent survival, with species and sites

**TABLE 1.** Locations and sampling effort in the 5 constant-effort mist-netting sites used in this study in Cusuco National Park, Honduras.

Site	Location	Elevation (m)	Years operational
Cantiles	15.516464, -88.243836	1,943	2012 to 2024
Base Camp	15.49785, -88.21279	1,595	2012 to 2024
El Danto	15.53044, -88.27602	1,522	2012 to 2019
El Cortecito	15.523186, -88.287458	1,375	2012 to 2019
Guanales	15.487356, -88.234386	1,350	2012 to 2024

as random effects—enables us to upscale demographic data analysis.

Here, we use Bayesian hierarchical multi-species reverse-symmetry CMR models to estimate demographic parameters for 17 bird species from a 12-yr constant-effort banding project in Cusuco National Park (CNP), Honduras. Evidence for upslope shifts in the avian community of CNP has previously been shown with long-term point count data (Neate-Clegg et al. 2018, 2021a) and, since 2012, constant-effort mist netting has been conducted along the same gradient, offering the potential to corroborate shifts and establish potential elevation-specific demographic mechanisms. We thus apply reverse-symmetry CMR models to these data to (1) estimate baseline demographic parameters, (2) investigate demographic parameters as a function of elevation, and (3) assess how temporal trends in demographic parameters vary with elevation. In addition, we used estimates from the models to test 2 predictions related to upslope range shifts: (1) that species found at lower elevations had higher population growth rates than species found at higher elevations and (2) that the difference in population growth rates between higher and lower sites reflected previously estimated upslope shift rates (Neate-Clegg et al. 2021a). Further, we demonstrate a framework for analyzing long-term demographic trends in tropical birds, collectively presenting an analytical pipeline to better understand demographic rates across spatial gradients.

## METHODS

### Field Site

All fieldwork was undertaken in Cusuco National Park (15.496°N, -88.212°E), in the Merendón Mountains, northwestern Honduras. The park is internationally recognized as one of the planet's most “irreplaceable” protected areas (Le Saout et al. 2013), characterized by high rates of regional endemism across multiple taxonomic groups (Martin et al. 2021). These mountains are typified by montane cloud forest, dominated by *Quercus* spp., *Pinus* spp., Lauraceae spp., and *Liquidambar styraciflua*, with elfin forest at the highest elevations (up to 2,242 m). Approximately 263 species of birds have been recorded in the park, 28.5% of which are endemic to the Mesoamerican Highlands biodiversity hotspot (Myers et al. 2000, Martin et al. 2021). The biological community of CNP has been extensively studied since 2004, via a series of permanent transects and research camps situated at different elevations (Martin et al. 2021).

### Constant Effort Mist-Netting

Mist-netting was undertaken during annual June–August field seasons between 2012 and 2024, in the form of standardized constant-effort sites (CES) (Robinson et al. 2009). Annual

field work co-occurred with the local breeding season, with birds typically breeding between May and July. In 2012, 7 CES sites were established at research camps across an elevational gradient of 820 to 1,943 m, all of which (bar 2) are in closed canopy primary/disturbed primary forest (some selective logging occurred around “Base Camp” in ~1950 prior to its gazetttement as a national park). Owing to logistical challenges, only 3 of these sites have been operated during all field campaigns since 2012, with a further 2 operated between 2012 and 2019. No fieldwork was undertaken in 2020/21, owing to the COVID-19 pandemic. For this study, we focused on the 5 primary forest sites that have been operated for the longest time (Table 1), ranging in elevation from 1,350 to 1,943 m. One of these 5 sites (El Danto) was re-opened in 2024 after a 5-year gap, but owing to this substantial time gap, we omitted 2024 data from this site from our analysis.

Each CES comprises 10 12-m (32-mm mesh) mist nets (Ecotone, Poland). Nets were opened between 0530 and 0600 hours and remained open for 6 hr from opening time. In incidences of later starts than this time, all sessions finished at 1200 hours. A full session thus comprised 60 net-hours, with any discrepancies from this total recorded (due to late opening of nets, nets not opened, or closures during the session). No mist-netting sessions were undertaken on rainy or windy mornings (although, occasionally, nets were closed during sessions owing to wind at Cantiles—the highest elevation site). The locations of the nets at each CES remained unchanged throughout the study period, with the exception of occasional minor shifts (within 10m) of net locations usually due to unmovable tree falls. The only exception to this was one site (El Cortecito) where net effort was reduced in 2017 onwards from 10 to 5 nets.

At each of the CES sites, we aimed for 6 mist-netting sessions in each field season, comprising 360 net hours total. These sessions (for each site, per season) were achieved by undertaking weekly pulses, where a given site was operated for 2 to 3 sessions in a week, each separated by at least one “rest” day. After a weekly pulse was undertaken at a given site, it was then rested for at least 1 week (but preferentially 2) before the next pulse. Rest days and weeks were incorporated into the protocol to avoid net shyness as much as possible. Sessions were typically operated by 2 trained banders, with all nets checked approximately every 40 min.

Upon capture, all birds were banded with appropriately sized, custom-made zinc-alloy bird bands (Porzana, Poland), with the exception of hummingbirds (Trochilidae), and very large species for which we did not have appropriately sized bands (e.g., *Zentrygon albifacies*). Ageing was attempted using the “WRP” cycle-based ageing system (Wolfe et al. 2010), but we elected to not include age-specific parameters in our models owing to inconsistency in use across banders

**TABLE 2.** Capture–mark–recapture parameters for 17 cloud-forest bird species in Cusuco National Park, Honduras. Presented for each species is the annual mean apparent survival probability ( $\phi$ ), recruitment rate ( $b$ ), realized population growth rate ( $\lambda$ ), capture probability ( $p$ ), and residency probability ( $r$ ), with associated standard deviation in parentheses. Capture probability is based on 6 mist-netting sessions. Also presented is the number of captures (year–individual combinations) and number of individuals (based on band ID). Species are presented in taxonomic order.

Species	Family	Captures	Individuals	$\phi$	$b$	$\lambda$	$p$	$r$
<i>Sclerurus mexicanus</i>	Furnariidae	38	33	0.64 (0.14)	0.39 (0.15)	1.03 (0.06)	0.28 (0.19)	0.68 (0.19)
<i>Sittasomus griseicapillus</i>	Furnariidae	49	30	0.82 (0.07)	0.22 (0.08)	1.04 (0.04)	0.46 (0.16)	0.66 (0.13)
<i>Xiphorhynchus erythropygius</i>	Furnariidae	31	24	0.85 (0.09)	0.25 (0.10)	1.09 (0.05)	0.15 (0.08)	0.84 (0.13)
<i>Anabacerthia variegaticeps</i>	Furnariidae	40	36	0.35 (0.15)	0.65 (0.15)	1.00 (0.04)	0.78 (0.60)	0.58 (0.22)
<i>Clibanornis rubiginosus</i>	Furnariidae	26	22	0.80 (0.13)	0.31 (0.14)	1.11 (0.07)	0.37 (0.24)	0.44 (0.21)
<i>Ceratopipra mentalis</i>	Pipridae	102	83	0.69 (0.09)	0.30 (0.09)	0.99 (0.03)	0.59 (0.22)	0.49 (0.11)
<i>Platyrinchus cancrominus</i>	Tyrannidae	24	19	0.58 (0.15)	0.37 (0.15)	0.95 (0.06)	0.37 (0.23)	0.71 (0.19)
<i>Mionectes oleagineus</i>	Tyrannidae	90	80	0.44 (0.13)	0.54 (0.13)	0.98 (0.03)	0.71 (0.41)	0.44 (0.18)
<i>Empidonax flavescens</i>	Tyrannidae	73	67	0.73 (0.13)	0.29 (0.13)	1.02 (0.03)	0.21 (0.15)	0.47 (0.21)
<i>Henicorhina leucophrys</i>	Troglodytidae	85	73	0.64 (0.11)	0.47 (0.11)	1.11 (0.04)	0.44 (0.22)	0.62 (0.17)
<i>Myadestes unicolor</i>	Turdidae	185	161	0.52 (0.08)	0.52 (0.08)	1.05 (0.02)	0.30 (0.12)	0.80 (0.13)
<i>Catharus frantzii</i>	Turdidae	23	16	0.53 (0.12)	0.32 (0.12)	0.85 (0.06)	0.55 (0.31)	0.78 (0.16)
<i>Catharus mexicanus</i>	Turdidae	222	156	0.68 (0.05)	0.33 (0.05)	1.01 (0.02)	0.56 (0.12)	0.66 (0.08)
<i>Chlorospingus flavopectus</i>	Passerellidae	152	125	0.66 (0.07)	0.34 (0.07)	1.00 (0.02)	0.27 (0.10)	0.74 (0.14)
<i>Arremon brunneinucha</i>	Passerellidae	155	110	0.7 (0.06)	0.26 (0.06)	0.96 (0.02)	0.52 (0.13)	0.62 (0.09)
<i>Basileuterus culicivorus</i>	Parulidae	33	29	0.61 (0.2)	0.51 (0.21)	1.12 (0.06)	0.85 (0.6)	0.43 (0.19)
<i>Myioborus miniatus</i>	Parulidae	83	69	0.57 (0.11)	0.36 (0.11)	0.93 (0.03)	0.44 (0.21)	0.55 (0.17)

and species—largely due to insufficient knowledge of molt strategies and ageing strategies of species in the earlier years of our study—that could introduce bias.

## Analysis

We initially filtered the species list (Table 2) to those with  $\geq 20$  captures and  $\geq 4$  recaptures (a recapture threshold established by Kaschube et al. 2022). For each species, we then constructed capture histories for all individuals (as identified by their unique band numbers), where a capture history is a sequence of 1s and 0s depending on whether an individual was captured in a particular year. These capture histories are the traditional input for CMR models such as Cormack–Jolly–Seber (Lebreton et al. 1992) and Pradel models (Pradel 1996).

For our analyses, we constructed CMR models in a Bayesian framework following Telenský et al. (2023). These models (hereafter “Telenský models”) assume 2 types of individuals: “transients” that are only passing through the site and are never again available for recapture, and “residents” that are available for future recapture, and in whose demographic properties we are interested. The input for these models requires converting capture histories into 2 “m-arrays” that inform the likelihood of the Telenský model:  $F$  (i.e., first captures) and  $R$  (i.e., recaptures). The  $F$  m-array summarizes first-capture data on both known residents (i.e., individuals captured in multiple years), as well as data on individuals of unknown residency status (i.e., individuals observed in only one year, which includes a mixture of residents and transients), while the  $R$  m-array summarizes subsequent captures of known residents. These arrays contain rows for each initial release occasion ( $t$ )—as well as any other grouping variables to be incorporated into models, such as sites or species—and columns representing sums of first recaptures (for  $F$ ) or subsequent recaptures (for  $R$ ), plus an additional column with sums of birds of each release occasion that were never recaptured (see Telenský et al. 2023 for more details).

The likelihood formulation of Telenský models includes 4 primary parameters: (1) apparent survival,  $\phi_t$ , the probability of an individual surviving and remaining in the population between time  $t$  and  $t + 1$  (i.e., estimated forward in time); (2) seniority,  $\gamma_t$ , the probability that an individual alive and in the population at time  $t$  was also alive and in the population at time  $t - 1$  (i.e., estimated backward in time, hence the “reverse symmetry”); (3) residency probability,  $r$ , the probability that an individual captured at time  $t$  is a resident; and (4) capture probability,  $p$ , the probability of capturing a resident that is alive and in the population at time  $t$ . We can then define prior probability models for each of these parameters, or define logit-linear models that allow the parameters to vary as functions of explanatory covariates. Under this parameterization, we can derive an estimate of the population growth rate,  $\lambda_t$  i.e., the proportional change in population size between  $t$  and  $t + 1$ , as

$$\lambda_t = \frac{\phi_t}{\gamma_{t+1}} \quad (1)$$

and the recruitment rate,  $b_t$  (i.e., the per capita rate of addition of new individuals to the population between  $t$  and  $t + 1$ ), where

$$b_t = \lambda_t - \phi_t = \frac{\phi_t}{\gamma_{t+1}} - \phi_t \quad (2)$$

These functional relationships allow rearrangement to define  $\gamma_t$ —which is of little direct biological interest—as a function of either  $b_t$  or  $\lambda_t$ , which then allows for the modeling of these parameters as functions of covariates. For example, if, instead of deriving  $b_t$ , we derive  $\gamma_t$  based on the relationship,  $\gamma_{t+1} = \phi_t / \lambda_t$ , we can then define a log-linear model for  $\lambda_t$ . Or, if we assign  $\gamma_{t+1} = \phi_t / (\phi_t + b_t)$ , we can then define a log-linear model for  $b_t$ .

Telenský models, which are implemented in a Bayesian context, have several advantages over traditional Pradel models.

First, regardless of which parameters we model directly, estimates and credible intervals of remaining parameters can be derived from plugging posterior distributions into the functional relationships defined above. Second, the generalized linear equations for any of the key parameters can include random effects such as species or site, a property absent from available frequentist implementations of CMR models such as program MARK (Cooch and White 2006). By including species random effects in multi-species models, we can then obtain inferences about community-level responses, as well as species-specific parameter estimates. These advantages are also true of other Bayesian formulations of Pradel models (Tenan et al. 2014). However, Telenský models have the additional advantage of accounting for the presence of transient individuals in samples (i.e., individuals with zero probability of being available at a site following initial capture; Pradel et al. 1997). Doing so can provide more ecologically relevant demographic estimates, unbiased by transient individuals, as well as a means of estimating and modeling residency probability, which may also be of ecological interest and provide additional insights into processes affecting the dynamics and demography of local populations (Telenský et al. 2023).

Here, we expand the Telenský models to estimate demographic parameters for each species,  $i$ , at each site,  $j$ . Although we preserve the likelihood formulation from Telenský et al. (2023), we model seniority in terms of apparent survival and recruitment (following the relationship in Equation 2), which are then modeled as a function of covariates. We conducted our analysis in R version 4.3.2 (R Core Team 2023) using the *nimble* package (de Valpine et al. 2017).

The first step of our CMR analysis was to estimate baseline demographic parameters for each species, pooled in a multi-species model. To do this, we used a simple model where  $\phi_i$ ,  $b_i$ , and  $r_i$  for species  $i$  were held constant over sites and time. Because the number of banding sessions at each site varied slightly from year to year (4 to 13, median = 6), we explicitly accounted for how this variation would affect capture probability,

$$p_{ijk} = 1 - (1 - p_i^*)^{\text{nsesh}_{jk}} \quad (3)$$

where the capture probability,  $p_{ijk}$ , for species  $i$  at site  $j$  in year  $k$  is equal to the probability of being captured in at least one banding session, where  $p_i^*$  is the species-specific capture probability for a single session, and  $\text{nsesh}_{jk}$  is the number of banding sessions at site  $j$  in year  $k$ . When reporting capture probabilities, we do so assuming 6 banding sessions (the median number), that is,  $1 - (1 - p_i^*)^6$ .

In this model, all species were treated as “fixed effects” in that the species-specific parameters ( $\phi_i$ ,  $b_i$ ,  $p_i^*$ , and  $r_i$ ) were assumed to be independent, being drawn separately from priors. We used vague priors for all parameters: Uniform (0, 1) for probabilities, and Uniform (0, 2) for recruitment rate. We ran the model for 20,000 iterations over 3 chains with a burn-in of 10,000 and 10-fold thinning. We confirmed model convergence based on the Gelman-Rubin convergence diagnostic, and also checked that parameter estimates were not tending towards the limits (0 or 1), which is a sign of failed convergence. Additionally, we performed posterior predictive checks to assess goodness-of-fit by simulating  $\mathbf{F}$  and  $\mathbf{R}$  arrays from the posterior distributions of the probability parameters of their multinomial models, calculating Freeman-Tukey statistics (Conn et al. 2018), and comparing the Freeman-Tukey statistics from the simulated data to those calculated from the

observed data to calculate Bayesian  $P$ -values. These Bayesian  $P$ -values were not significant ( $\mathbf{F}$ :  $P = 0.84$ ;  $\mathbf{R}$ :  $P = 0.87$ ), indicating that the models provided adequate fit for this dataset. From this model we then extracted the mean and 95% credible intervals of the posteriors for each parameter. We then calculated estimates of  $\lambda_i$  by summing the posteriors of  $\phi_i$  and  $b_i$ , propagating the uncertainty.

In the second step, we were interested in whether demographic rates varied with elevation. As this step requires sufficient capture and recapture data across a range of sites, we filtered the species set to those with  $\geq 50$  individuals, where each species was captured at  $\geq 4$  sites with  $\geq 5$  captures per site (Table 3). We defined models for apparent survival and recruitment as

$$\text{logit}(\phi_{ij}) = \alpha_{\phi_i} + \beta_{\phi_i} \cdot \text{elev}_j \quad (4)$$

$$\log(b_{ij}) = \alpha_{b_i} + \beta_{b_i} \cdot \text{elev}_j \quad (5)$$

where both parameters are modeled (on the logit/log scale, respectively) as a function of an intercept,  $\alpha$ , representing the mean species-specific demographic rate, and a slope,  $\beta$ , representing the species-specific effect of elevation on the demographic rate. Elevation was centered to have a mean of 0 and divided by 100 to render the slope coefficients in terms of each 100-m deviation in elevation. Similarly, we also modeled residency,

$$\text{logit}(r_{ij}) = \alpha_{r_i} + \beta_{r_i} \cdot \text{elev}_j \quad (6)$$

as a function of elevation.

In this model, species were treated as “random effects” for all demographic rates, where all the species-specific intercept and slope parameters were modeled following:

$$\alpha_{\phi_i} \sim \text{Normal}(\mu_{\alpha_{\phi}}, \sigma_{\alpha_{\phi}}) \quad (7)$$

$$\beta_{\phi_i} \sim \text{Normal}(\mu_{\beta_{\phi}}, \sigma_{\beta_{\phi}}) \quad (8)$$

whereby species effects were drawn from normal distributions with hyperparameters governing the cross-species means and variances. As with the previous model, we used vague priors (now including Normal (0, 10) for slopes, and Gamma (1, 1) for standard deviations), and ran this model for 20,000 iterations over 3 chains with a burn-in of 10,000 and ten-fold thinning, and the posterior predictive checks (Freeman-Tukey tests, as defined above) were not significant ( $\mathbf{F}$ :  $P = 0.65$ ;  $\mathbf{R}$ :  $P = 0.88$ ). From this model, we extracted the means and credible intervals of all parameters, as well as the proportion of posteriors  $> 0$  or  $< 0$  as a measure of the strength of evidence. We also used the posteriors of  $\phi_{ij}$  and  $b_{ij}$  to calculate estimates of  $\lambda_{ij}$ , propagating the uncertainty.

In the third step, we wanted to test whether temporal trends in apparent survival, recruitment, and residency probability varied by elevation. We modeled all 3 demographic parameters as a function of elevation, year, and their interaction:

$$\text{logit}(\phi_{ijk}) = \alpha_{\phi_i} + \beta_{\phi_i} \cdot \text{elev}_j + \theta_{\phi_i} \cdot \text{year}_k + \zeta_{\phi_i} \cdot \text{elev}_j \cdot \text{year}_k \quad (9)$$

$$\log(b_{ijk}) = \alpha_{b_i} + \beta_{b_i} \cdot \text{elev}_j + \theta_{b_i} \cdot \text{year}_k + \zeta_{b_i} \cdot \text{elev}_j \cdot \text{year}_k \quad (10)$$

$$\text{logit}(r_{ijk}) = \alpha_{r_i} + \beta_{r_i} \cdot \text{elev}_j + \theta_{r_i} \cdot \text{year}_k + \zeta_{r_i} \cdot \text{elev}_j \cdot \text{year}_k \quad (11)$$

**TABLE 3.** Effects of elevation on the demographic parameters of 6 cloud-forest bird species in Cusuco National Park, Honduras. Presented for each species are the model parameters (Equations 4–6) for the effects of elevation ( $\beta$ ) on residency probability ( $r$ ), apparent survival probability ( $\varphi$ ) and recruitment rate ( $b$ ). Each parameter is associated with its 95% Bayesian credible interval, as well as the proportion of posteriors  $> 0$ . Species are presented in taxonomic order.

Species	Parameter	Estimate	2.5%	97.5%	Pr (> 0)
<i>Henicorhina leucophrys</i>	$r$	0.04	-0.51	0.72	0.54
	$\varphi$	-0.01	-0.20	0.17	0.48
	$b$	0.01	-0.09	0.10	0.54
<i>Myadestes unicolor</i>	$r$	0.19	-0.23	0.87	0.76
	$\varphi$	-0.02	-0.17	0.14	0.43
	$b$	0.01	-0.08	0.10	0.55
<i>Catharus mexicanus</i>	$r$	-0.19	-0.73	0.29	0.23
	$\varphi$	0.04	-0.12	0.22	0.68
	$b$	0.02	-0.08	0.11	0.63
<i>Chlorospingus flavopectus</i>	$r$	0.51	-0.12	2.01	0.89
	$\varphi$	0.05	-0.12	0.22	0.72
	$b$	0.00	-0.09	0.10	0.53
<i>Arremon brunneinucha</i>	$r$	0.09	-0.28	0.58	0.65
	$\varphi$	-0.05	-0.20	0.10	0.28
	$b$	-0.01	-0.12	0.08	0.40
<i>Myioborus miniatus</i>	$r$	0.21	-0.23	0.91	0.77
	$\varphi$	0.03	-0.12	0.19	0.62
	$b$	0.00	-0.11	0.10	0.51

Capture probability was modeled following Equation (3). All intercepts and slopes, including the interaction term, were again modeled with species-specific random effects as above. Model priors and settings followed the previous models and the posterior predictive checks were not significant (F:  $P = 0.55$ ; R:  $P = 0.76$ ). From this model we extracted the means and credible intervals of all parameters and used the posteriors of  $\phi_{ijk}$  and  $b_{ijk}$  to calculate estimates of  $\lambda_{ijk}$ , propagating the uncertainty.

### Relating Population Growth Rates to Elevational Position and Shifts

To assess whether demographic rates are related to upslope shifts (Neate-Clegg and Tingley 2023), we investigated 2 predictions. First, we tested whether species typically found at lower elevations had higher population growth rates than species typically found at higher elevations, because lower elevation species expanding upslope into our sites should exhibit population increases, while the trailing edge of high elevation species should exhibit population declines (Neate-Clegg et al. 2021b). To test this prediction, we first calculated the mean elevation of all the captured individuals of each species. Then, for every posterior of the first model, we regressed the estimated population growth rates of each species against their mean elevations, thus propagating the uncertainty in the population growth rates. Across these 3,000 iterations, we calculated the mean regression coefficient and 95% credible intervals.

Second, to assess whether the effect of elevation on population growth rates could be related to elevational shift rates (m/year), we extracted previously published shift rate estimates (Neate-Clegg et al. 2021a) for the subset of species included in the second CMR model. We estimated the effect of elevation on population growth rates by subtracting the population growth rate of the second-lowest sites (as

one species was not represented at the lowest site) from that of the highest elevation site, and repeated this for every posterior draw of the second model. Positive and negative values thus indicated increased and decreased growth rates with elevation, respectively. Then, for every posterior, we regressed the difference in population growth rates against the elevational shift rates, propagating the uncertainty in the population growth rates. Across these 3,000 iterations, we calculated the mean regression coefficient and 95% credible intervals. Given the few species for which we were able to fit this model, we note that the results are inherently preliminary.

## RESULTS

### Overall Demographic Rates

Our 12-year dataset from 5 focal sites comprised 3,329 captures of 74 species. Seventeen species from 7 families had sufficient data to estimate baseline demographic parameters (Figure 1, Table 2). Annual capture probabilities (assuming 6 banding sessions per year) ranged from 0.15 (*Xiphorhynchus erythropygius*) to 0.85 (*Basileuterus culicivorus*). Residency probability ranged from 0.43 (*Basileuterus culicivorus*) to 0.84 (*Xiphorhynchus erythropygius*). Apparent survival estimates ranged from 0.35 (*Anabacerthia variegaticeps*) to 0.85 (*Xiphorhynchus erythropygius*). Recruitment estimates ranged from 0.22 (*Sittasomus griseicapillus*) to 0.65 (*Anabacerthia variegaticeps*). Realized population growth rates ranged from 0.85 (*Catharus frantzii*) to 1.12 (*Basileuterus culicivorus*). When comparing population growth rates to the mean elevation of each species, there was fairly strong evidence that population growth rates were lower for species captured at higher elevations (Figure 2A; mean coefficient = -0.01 change per 100 m elevation, 95% Bayesian credible interval (95% CrI): -0.027 to 0.005; Pr (coefficient < 0) = 91%).

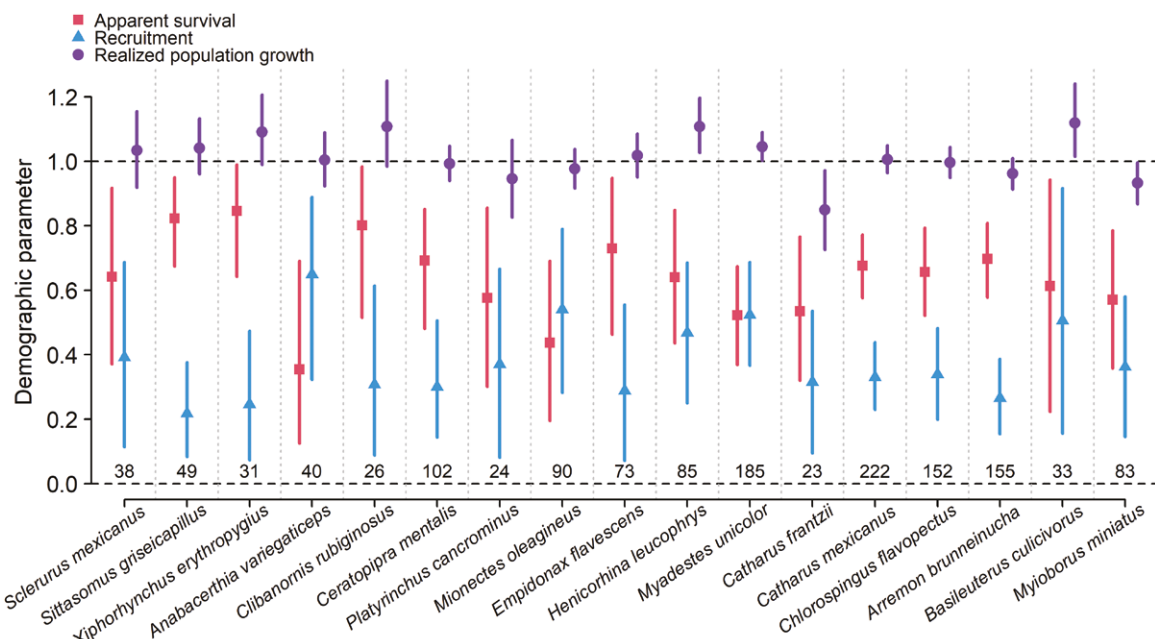


**FIGURE 1.** Baseline demographic parameters for 17 cloud-forest bird species in Cusuco National Park, Honduras. Each point represents the mean apparent survival probability ( $\varphi$ ), recruitment rate ( $b$ ), and realized population growth rate ( $\lambda$ ) for each species, and bars show the 95% Bayesian credible intervals. Numbers below give the sample size (number of captures) for each species. The upper dashed line indicates a population growth rate of 1 (i.e., a stable population).

### Elevation-Specific Demographic Rates

Of the 17 species, 6 (Table 3) had sufficient data to investigate the effects of elevation on demographic parameters (Figure 3A). There was little evidence that average residency probability varied with elevation ( $\mu_{\beta_r} = 0.14$ , 95% CrI: -0.33 to 0.79;  $\text{Pr}(\mu_{\beta_r} > 0) = 70\%$ ). There was also no evidence that apparent survival ( $\mu_{\beta_\varphi} = 0.006$ , 95% CrI: -0.14 to 0.16;  $\text{Pr}(\mu_{\beta_\varphi} > 0) = 54\%$ ) or recruitment varied with elevation ( $\mu_{\beta_b} = 0.003$ , 95% CrI: -0.09 to 0.09;  $\text{Pr}(\mu_{\beta_b} > 0) = 51\%$ ). Combined, this led to little change in population growth rates, albeit with a slight increase toward higher elevations.

At the species level (Figure 3B–G), no species showed strong changes in residency probability with elevation, although *Chlorospingus flavopectus* showed a trend towards residency increasing with elevation (Table 3). No species showed evidence of elevational differences in apparent survival or recruitment (Table 3). Despite the lack of strong trends in apparent survival and recruitment, weak trends in the population growth rates of some species were evident (Figure 3B–G). Of the 6 species, 3 in particular showed a trend towards increasing population growth rates with increasing elevation, resulting from the additive effects of positive elevational trends in both survival and recruitment. Furthermore, *Cathartes mexicanus*, one of the species with the largest sample sizes, showed some evidence (Figure 3D) that population growth rates were  $> 1$  at higher elevations ( $\text{Pr}(\lambda > 1) = 91\%$ ) and  $< 1$  at the lowest elevations ( $\text{Pr}(\lambda < 1) = 79\%$ ).

Change in population growth rates across elevation was positively associated with elevational shift rates across the 6 species (Figure 2B; mean coefficient = 0.023, 95% CrI: 0.001 to 0.049;  $\text{Pr}(\text{coefficient} > 0) = 98\%$ ), and consistent (e.g., positive effect of elevation on population growth rates, positive change in mean elevation over time) for 5 out of 6 species, indicating that upslope shifts were associated with higher population growth rates at higher elevations.

### Temporal Trends in Demographic Rates

We found fairly strong evidence ( $\mu_{\theta_r} = -0.48$ , 95% CrI: -1.28 to 0.25;  $\text{Pr}(\mu_{\theta_r} < 0) = 90\%$ ) that residency probability decreased over time, as well as strong evidence for an interaction between time and elevation ( $\mu_{\zeta_r} = 0.27$ , 95% CrI: -0.04 to 0.54;  $\text{Pr}(\mu_{\zeta_r} > 0) = 96\%$ ), where decreases in residency were less pronounced at higher elevations. There was strong evidence ( $\mu_{\theta_\varphi} = 0.46$ , 95% CrI: 0.02 to 0.92;  $\text{Pr}(\mu_{\theta_\varphi} > 0) = 98\%$ ) that apparent survival increased over time (Figure 4), as well as strong evidence for an interaction between time and elevation ( $\mu_{\zeta_\varphi} = -0.16$ , 95% CrI: -0.36 to 0.03;  $\text{Pr}(\mu_{\zeta_\varphi} < 0) = 96\%$ ), such that increases were lower at higher elevations, to the point that survival decreased over time at the highest elevation site. Conversely, there was also strong evidence ( $\mu_{\theta_b} = -0.50$ , 95% CrI: -0.83 to -0.14;  $\text{Pr}(\mu_{\theta_b} < 0) = 99.5\%$ ) of a decrease in recruitment over time (Figure 4), again with strong evidence for an interaction ( $\mu_{\zeta_b} = 0.11$ , 95% CrI: -0.01 to 0.26;  $\text{Pr}(\mu_{\zeta_b} > 0) = 97\%$ ), such that recruitment was fairly stable at the highest elevation site. The combined effect of time and elevation on demographic rates was that population growth rates decreased at most elevations (Figure 4).

For residency probability at the species level (Table 4), all species had negative time coefficients with at least fairly strong evidence (i.e.,  $\text{Pr}(\theta_{ri} < 0) = 84\text{--}97\%$ ) for 4 species, while all species had positive interaction coefficients with at least fairly strong evidence ( $\text{Pr}(\zeta_{ri} > 0) = 86\text{--}99\%$ ). For these species, residency probability decreased over time, and more so at lower elevations. For apparent survival (Table 4), all species had positive time coefficients with at least fairly strong evidence ( $\text{Pr}(\theta_{\varphi i} > 0) = 87\text{--}100\%$ ), and all species had a negative interaction coefficient with at least fairly strong evidence ( $\text{Pr}(\zeta_{\varphi i} < 0) = 81\text{--}98\%$ ). For these species, apparent survival increased over time more at lower elevation sites than higher elevation sites, with survival actually decreasing at the

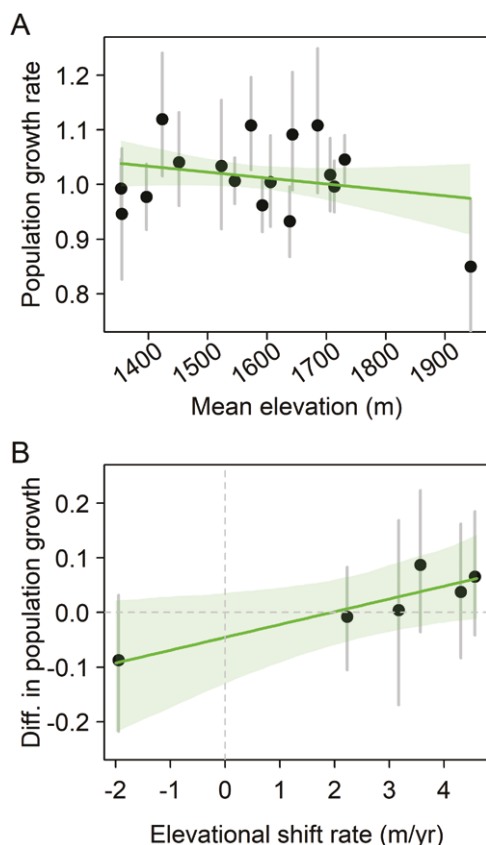


**FIGURE 2.** Relationships between population growth rates, elevational position, and elevational shift rates for cloud-forest bird species. Mean population growth rates (A) for 17 species were negatively associated with the mean elevation at which each species was captured. The difference in population growth rates between high and low elevation sites for 6 species (B) was positively associated with previously estimated elevational shift rates. The trend lines and ribbons show the mean effect and 95% Bayesian credible intervals, whereas the vertical bars show the credible intervals for the point estimates.

highest site for 5 species (Figure 4). For recruitment (Table 4), all species had negative time coefficients with strong evidence (i.e.,  $\text{Pr}(\theta_{bi} < 0) = 98\text{--}100\%$ ), as well as positive interaction coefficients with at least fairly strong evidence (i.e.,  $\text{Pr}(\zeta_{bi} > 0) = 88\text{--}98\%$ ). For these species, recruitment tended to decrease over time more at lower elevation sites, with weaker trends at the highest site. Taken together, population growth rates declined the most at higher elevation sites but still remained higher overall than lower elevation sites for all species, with the lowest sites seeing population declines for at least 4 out of 6 species by the end of the study.

## DISCUSSION

Long-term monitoring is essential to both track and understand population dynamics and the potential mechanisms driving observed population changes. We present trends suggesting that the demographic rates of several cloud-forest bird species in Honduras vary over time and with elevation (Figures 3 and 4), with some species showing population declines, and others increases (Figure 1). At the species level there was weak evidence (Figure 3) that some populations were increasing at higher elevations ( $\lambda > 1$ ) and decreasing at lower elevations ( $\lambda < 1$ ), especially towards the end of the

study period (Figure 4), broadly consistent with the hypothesis that species are shifting upslope over time (Neate-Clegg et al. 2021a, Freeman et al. 2021). This was particularly the case for *Catharus mexicanus*, one of the most represented species in our dataset (Table 3, Figure 3D). Although more years of data are necessary to robustly establish confidence in these trends, the analytical framework we have outlined will facilitate efficient re-analysis in the future.

Despite the small sample size, our results are nonetheless suggestive of some populations growing at the leading (upper) edge of their elevational ranges, while concurrently decreasing at the (lower) trailing edge. Such trends are consistent with previous findings in CNP—that the distributions of many cloud-forest species are moving upslope (Neate-Clegg et al. 2018). Indeed, we found fairly strong evidence that, across 17 species, average population growth rates were negatively associated with the elevational position of each species (Figure 2A), suggesting that lower elevation species have increased at our sites as they shift upslope, while higher elevation species declined at their trailing edge. This pattern has also been reported in Tanzania, and the Himalayas (Neate-Clegg et al. 2021b, Srinivasan and Wilcove 2021), lending support to the use of basic demographic rates in conjunction with elevational ranges to infer range shifts. Moreover, the change in population growth rates with elevation was positively associated with the shift rate estimates of Neate-Clegg et al. (2021a) and consistent in sign for 5 out of 6 species (Figure 2B), albeit a small sample size. Yet, given that these elevational shift rates were estimated from a different data source (point counts) within the same system, our result suggests that the effect of elevation on population growth rates could be a good indicator of elevational shifts.

For the species whose population growth rates tended to increase with elevation (e.g., *Catharus mexicanus*, *Chlorospingus flavopectus*), these patterns were generally mirrored by increases in both apparent survival and recruitment rate across elevation (Figure 3). The similarities in these relationships suggest that increased population growth rates at higher elevations could be driven by both higher survival and higher recruitment rates, indicative of a mechanistic role in mediating elevational shifts. For example, population decreases at lower elevations could be driven by increases in nest predation rates (Boyle 2008, Cox et al. 2013, Londoño et al. 2023), while increases in survival or recruitment at higher elevations could be mediated by more favorable ecological conditions or resources as a result of warming, particularly for species near the upper edge of their elevational distribution (Rubenstein et al. 2023). Nevertheless, the same processes may also apply to species shifting downslope, such as *Arremon brunneinucha*, that had higher survival as well as higher recruitment at lower elevations.

Temporal trends in demographic rates (Figure 4) indicated that apparent survival tended on average to increase over time, while recruitment decreased. Overall, this led to declines in population growth rates at the multi-species level. However, these temporal trends varied somewhat by species and elevation (Table 4), being stronger at lower elevations with the consequence that, at the highest elevation site, apparent survival actually decreased over time for 5 species while the recruitment rate was stable for most species (Figure 4). Recruitment could be decreasing at lower elevations due to factors such as negative physiological effects, increased nest predation rates, or poor chick provisioning (Boyle 2008, Cox et al. 2013, Londoño et al. 2017, 2023), and these results corroborate findings from

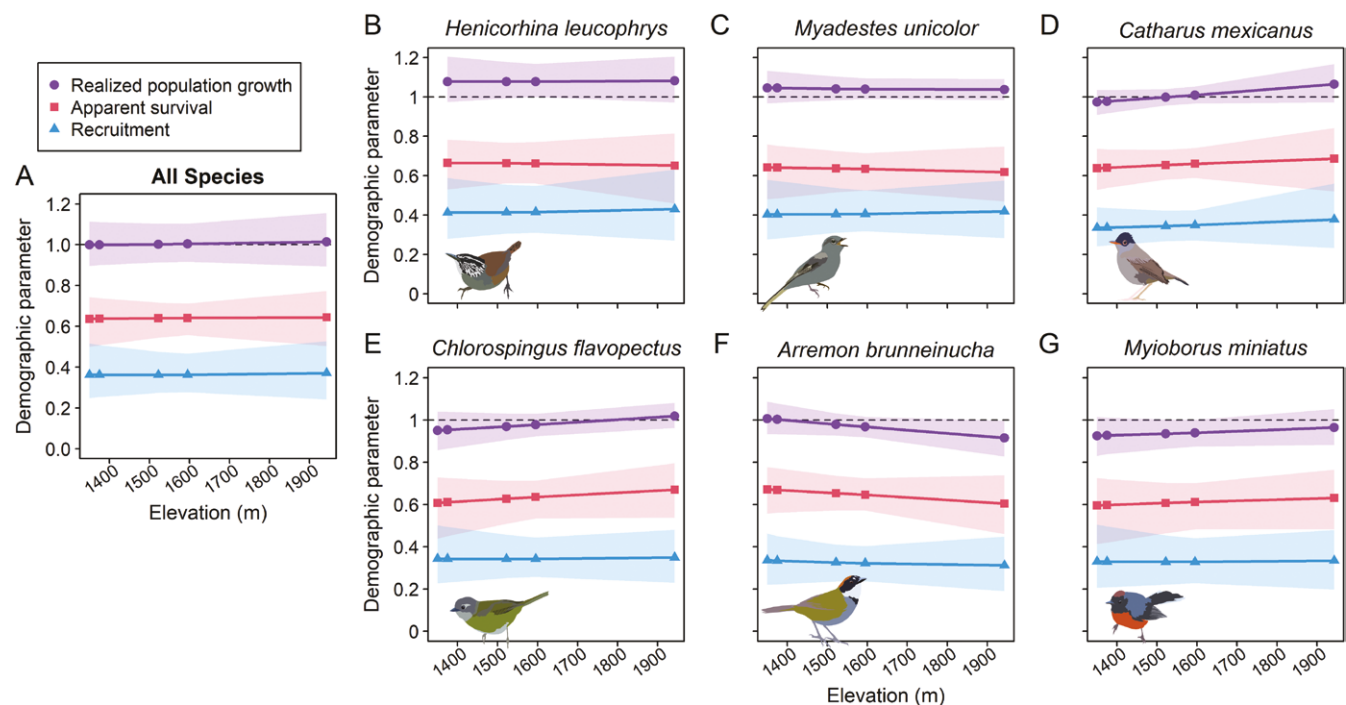


**FIGURE 3.** Variation in demographic parameters as a function of elevation for 6 cloud-forest bird species. For all species together (A), and for each species individually (B–G), lines show how apparent survival probability ( $\varphi$ ), recruitment rate ( $b$ ), and realized population growth rate ( $\lambda$ ) vary with elevation, with associated 95% Bayesian credible intervals. Points indicate the elevations of the five study sites. Dashed line indicates a population growth rate of 1 (i.e., a stable population).

other tropical sites that implicate recruitment decreases as a driver of population declines (Blake and Loiselle 2015, Brawn et al. 2017, Neate-Clegg et al. 2021b). As long-lived species at the slower end of the life-history continuum, cloud-forest birds are likely to favor their own survival over offspring provisioning (Ghalambor and Martin 2001). The fact that species at the highest elevation site showed fairly stable recruitment and survival suggests that these populations are yet to experience the same pressures as lower elevation populations. However, with our study only spanning 12 years, the temporal dynamics observed might not reflect multi-decadal trends (Neate-Clegg et al. 2020), an issue with fitting linear trends to shorter time series (McCain et al. 2016, White 2019). It is also possible that our sites do not span a sufficient elevational gradient to fully capture the range of population dynamics, especially for species whose elevational ranges go below that of the lowest site in this study.

Besides the spatiotemporal variation in demographic rates, we also provide baseline estimates for 4 key demographic parameters for 17 species (Table 2), to our knowledge the first study to do so for Neotropical cloud-forest birds (but see studies on apparent survival e.g., Rangel-Salazar et al. 2008, Taylor and Komar 2010, Scholer et al. 2019). This is especially important as tropical montane birds may exhibit differing demographic rates compared to their lowland counterparts (Scholer et al. 2019). Apparent survival was higher than the recruitment rate for most species (Figure 1), consistent with the slow-paced life-history strategies of tropical birds (Martin 2004, Wiersma et al. 2007, Scholer et al. 2020). Yet, even within this small set of species inhabiting the same mountain range, we saw notable variation in demographic rates, with signs that some species are increasing in population size while others are decreasing (Table 2, Figure 1). Notably, *Catharus*

*frantzii*, a high-elevation thrush, exhibited the lowest population growth rate, potentially the result of upslope shifts of its lower-elevation congener, *Catharus mexicanus*, to which it is competitively subordinate (Jones et al. 2019).

Our knowledge of the demographics of tropical birds is limited (Sheldon 2019), although an increasing number of studies are contributing to our understanding of tropical bird life history (Ruiz-Gutiérrez et al. 2012, Scholer et al. 2020, França et al. 2023). Within the tropics, most demographic studies to date have focused on lowland bird species (e.g., Ruiz-Gutiérrez et al. 2012, Wolfe et al. 2015, Brawn et al. 2017, Woodworth et al. 2018), with less attention paid to the hyper-diverse and range-restricted species of elevational gradients (but see: Scholer et al. 2019, Kittelberger et al. 2021, Srinivasan and Wilcove 2021, Neate-Clegg et al. 2023). Moreover, many previous studies have not accounted for the presence of transient individuals, which could lead to underestimates of apparent survival probability, especially as apparent survival cannot directly separate emigration from true survival. Following Telenský et al. (2023) and others (e.g., Pradel et al. 1997, Hines et al. 2003, Saracco et al. 2010, França et al. 2023), we advocate for models that explicitly incorporate transient individuals so that survival and recruitment rates more accurately reflect that of resident birds. As studies reporting basic demographic rates increases, our ability to investigate large biogeographical and ecological patterns in life history continues to improve (Scholer et al. 2020, França et al. 2023). These studies will also provide baseline data that enable future comparisons (Kittelberger et al. 2021), allowing for more powerful interrogation of anthropogenic impacts on species-specific demographic rates.

With demographic data spanning 12 years, our study surpasses the oft-recommended 10-yr threshold for CMR

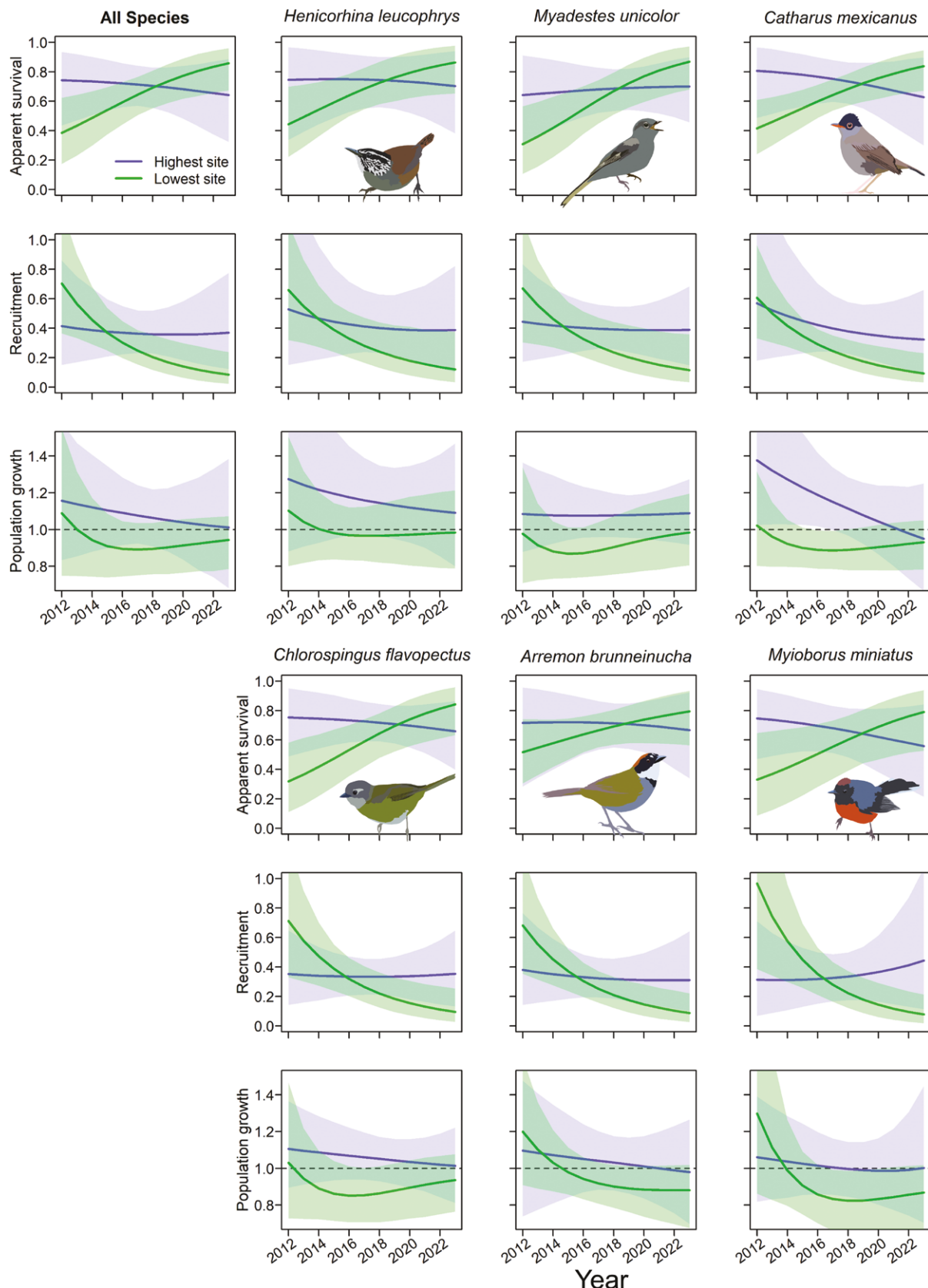


**FIGURE 4.** Variation in demographic parameters as a function of elevation and year for 6 cloud-forest bird species. For all species together, and for each species individually, lines show how apparent survival probability ( $\varphi$ ), recruitment rate ( $b$ ), and realized population growth rate ( $\lambda$ ) vary over time, with separate lines and 95% Bayesian credible intervals for the highest site (1,943 m) and lowest site (1,350 m). For *Henicorhina leucophrys*, the lowest site displayed is as at 1,375 m. For population growth rates, the dashed line indicates a population growth rate of 1 (i.e., a stable population).

**TABLE 4.** Effects of elevation, year, and their interaction on the demographic parameters of 6 cloud-forest bird species in Cusuco National Park, Honduras. Presented for each species are the model parameters [Equations 9–11] for the effects of elevation ( $\beta$ ), year ( $\theta$ ), and their interaction ( $\zeta$ ) on apparent survival probability ( $\varphi$ ), recruitment rate ( $b$ ), and residency probability ( $r$ ). Each parameter is associated with its 95% Bayesian credible interval, as well as the proportion of posteriors  $> 0$ . Species are presented in taxonomic order.

Species	Parameters	$\varphi$			$b$			$r$					
		Estimate	2.5%	97.5%	Pr (> 0)	Estimate	2.5%	97.5%	Pr (> 0)	Estimate	2.5%	97.5%	Pr (> 0)
<i>Henicorhina leucophrys</i>	$\beta$	0.02	-0.17	0.20	0.61	0.09	-0.04	0.20	0.93	-0.04	-0.46	0.41	0.41
	$\theta$	0.49	-0.04	1.14	0.96	-0.46	-0.81	-0.03	0.02	-0.70	-1.73	0.20	0.07
	$\zeta$	-0.15	-0.40	0.11	0.09	0.09	-0.08	0.24	0.88	0.32	-0.03	0.68	0.96
<i>Myadestes unicolor</i>	$\beta$	0.01	-0.14	0.16	0.57	0.09	-0.03	0.20	0.94	0.08	-0.22	0.56	0.63
	$\theta$	0.71	0.19	1.37	1.00	-0.45	-0.81	-0.02	0.02	0.02	-0.87	-1.90	0.03
	$\zeta$	-0.16	-0.36	0.04	0.06	0.11	-0.02	0.24	0.95	0.33	0.04	0.62	0.98
<i>Cathartes mexicanus</i>	$\beta$	0.05	-0.12	0.22	0.71	0.10	-0.01	0.21	0.96	-0.16	-0.61	0.18	0.20
	$\theta$	0.35	-0.05	0.75	0.96	-0.52	-0.86	-0.19	0.00	-0.43	-1.05	0.16	0.08
	$\zeta$	-0.19	-0.41	0.02	0.04	0.08	-0.07	0.22	0.88	0.23	-0.04	0.48	0.96
<i>Chlorostreingus flavpectus</i>	$\beta$	0.06	-0.10	0.25	0.75	0.07	-0.04	0.17	0.91	0.17	-0.21	1.04	0.70
	$\theta$	0.54	0.08	1.07	0.99	-0.49	-0.82	-0.08	0.01	-0.45	-1.38	0.50	0.16
	$\zeta$	-0.19	-0.42	0.00	0.02	0.13	0.00	0.26	0.98	0.21	-0.30	0.56	0.86
<i>Arremon brunneinucha</i>	$\beta$	0.02	-0.15	0.18	0.61	0.07	-0.06	0.17	0.91	0.00	-0.30	0.35	0.48
	$\theta$	0.28	-0.28	0.72	0.87	-0.52	-0.88	-0.17	0.00	-0.18	-0.89	0.55	0.30
	$\zeta$	-0.10	-0.32	0.18	0.19	0.11	-0.02	0.25	0.96	0.35	0.05	0.64	0.99
<i>Myiothlypis miniatus</i>	$\beta$	0.04	-0.11	0.22	0.70	0.07	-0.06	0.17	0.89	0.08	-0.30	0.65	0.60
	$\theta$	0.40	-0.21	0.96	0.92	-0.56	-1.02	-0.02	0.00	-0.16	-1.16	0.85	0.38
	$\zeta$	-0.19	-0.43	0.01	0.03	0.18	0.01	0.39	0.98	0.18	-0.18	0.46	0.86

research (Ruiz-Gutiérrez et al. 2012), yet it is still on the shorter end of long-term monitoring programs, shorter, indeed, than the lifespan of many tropical bird species (Valcu et al. 2014, Pollock et al. 2024). Nonetheless, using these analytical tools, the same analysis can be re-applied to our study system in the future to interrogate trends over longer time periods. We thus encourage others to employ the multi-species framework outlined here, allowing the simultaneous estimation of demographic rates across a bird community (Saracco et al. 2022), and the incorporation of hierarchical random effects (Tenan et al. 2014) in a Bayesian context.

As monitoring datasets mature around the tropics, we encourage ecologists to use our modeling approach, and those in Telenský et al. (2023), to estimate demographic rates in other systems to improve data availability. We also encourage pluralistic approaches that combine different datasets for greater inference. For example, we have demonstrated that demographic datasets from bird banding can be paired with alternative data from point counts (Neate-Clegg et al. 2018) to increase understanding of elevational patterns. In addition to recapture data, more comprehensive documentation of nest survival rates (Londoño et al. 2023) and ageing of immature birds (Johnson and Wolfe 2016, Pyle et al. 2022) could provide further inference on population dynamics across elevational gradients. The effects of climate change on birds are likely mediated by multiple influences, not least biotic factors (Jankowski et al. 2012, Neate-Clegg and Tingley 2023), and projects that relate demographic rates to a series of factors (e.g., resource availability, predation and parasitism rates, or interspecific competition) are needed to understand how global change is mechanistically integrated into population dynamics. We thus encourage holistic monitoring programs that incorporate multiple features of complex tropical systems likely to be intrinsically linked to avian population dynamics.

## Supplementary material

Supplementary material is available at *Ornithological Applications* online.

## Acknowledgements

We thank the many seasonal field staff who have worked in Cusuco National Park as part of annual fieldwork monitoring the avifauna of Cusuco for over a decade. We owe particular thanks to Operation Wallacea who facilitated fieldwork here, making this long-term monitoring possible. In particular, we are grateful to Steve Green, Declan Crace, Manuel Cruz, Tom Martin, Oliver Burdekin, and Merlin Jocqué for their help in design and logistics, in addition to a large team of local forest guides and other logistical staff who either accompanied us on surveys in the field, or facilitated our work here. We also thank Expediciones y Servicios Ambientales de Cusuco, particularly Roberto Downing, for their continued logistical service.

## Ethics statement

Bird banding/handling was performed under annual permits issued by Instituto de Conservación Forestal, and followed the protocols, training, and ethical standards of the British Trust for Ornithology bird ringing scheme.

## Conflict of interest statement

None declared.

## Author contributions

M.H.C.N.C. and S.E.I.J. conceived the idea, design, experiment (supervised research, formulated question or hypothesis). S.E.I.J., F.R.V., and M.H.C.N.C. performed the experiments (collected data, conducted the research). M.H.C.N.C., S.E.I.J., F.R.V., and J.F.S. wrote the paper (or substantially edited the paper). F.R.V. did the Spanish translation using DeepL Translator software and proofread it. M.H.C.N.C. and J.F.S. developed or designed methods. M.H.C.N.C. analyzed the data. S.E.I.J. and F.R.V. contributed substantial materials, resources, or funding.

## Data availability

All data and code supporting the analyses are freely available on FigShare at <https://doi.org/10.6084/m9.figshare.27199077.v1>

## LITERATURE CITED

Beissinger, S. R., and E. A. Riddell (2021). Why are species traits weak predictors of range shifts? *Annual Review of Ecology, Evolution, and Systematics* 52:47–66.

Blake, J. G., and B. A. Loiselle (2015). Enigmatic declines in bird numbers in lowland forest of eastern Ecuador may be a consequence of climate change. *PeerJ* 3:e1177.

Boyle, W. A. (2008). Can variation in risk of nest predation explain altitudinal migration in tropical birds? *Oecologia* 155:397–403.

Brawn, J. D., T. J. Benson, M. Stager, N. D. Sly, and C. E. Tarwater (2017). Impacts of changing rainfall regime on the demography of tropical birds. *Nature Climate Change* 7:133–136.

Briscoe, N. J., D. Zurell, J. Elith, C. König, G. Fandos, A. K. Malchow, M. Kéry, H. Schmid, and G. Guillera-Arroita (2021). Can dynamic occupancy models improve predictions of species' range dynamics? A test using Swiss birds. *Global Change Biology* 27:4269–4282.

Conn, P. B., D. S. Johnson, P. J. Williams, S. R. Melin, and M. B. Hooten (2018). A guide to Bayesian model checking for ecologists. *Ecological Monographs* 88:526–542.

Cooch, E. G., and G. C. White (2006). *Program MARK: a Gentle Introduction*, 17th edition. Colorado State University, Fort Collins, CO, USA.

Cox, W. A., F. R. Thompson, and J. L. Reidy (2013). The effects of temperature on nest predation by mammals, birds, and snakes. *The Auk* 130:784–790.

Forero-Medina, G., J. Terborgh, S. J. Socolar, and S. L. Pimm (2011). Elevational ranges of birds on a tropical montane gradient lag behind warming temperatures. *PLoS One* 6:e28535.

França, L. F., C. C. de Oliveira e Silva, J. B. de Pinho, N. P. Prestes, V. R. Cueto, M. A. S. Alves, F. Schunck, C. S. Fontana, C. Lugarini, J. Martinez, M. C. Sagario, et al. (2023). Similar regional-scale survival of tropical and southern temperate birds from the New World. *Oecologia* 202:239–250.

Freeman, B. G., and A. M. Class Freeman (2014). Rapid upslope shifts in New Guinean birds illustrate strong distributional responses of tropical montane species to global warming. *Proceedings of the National Academy of Sciences USA* 111:4490–4494.

Freeman, B. G., M. N. Scholer, V. Ruiz-Gutierrez, and J. W. Fitzpatrick (2018). Climate change causes upslope shifts and mountaintop extirpations in a tropical bird community. *Proceedings of the National Academy of Sciences USA* 115:11982–11987.

Freeman, B. G., Y. Song, K. J. Feeley, and K. Zhu (2021). Montane species track rising temperatures better in the tropics than in the temperate zone. *Ecology Letters* 24:1697–1708.

Ghalambor, C. K., and T. E. Martin (2001). Fecundity-survival trade-offs and parental risk-taking in birds. *Science* 292:494–497.

Hines, J. E., W. L. Kendall, and J. D. Nichols (2003). On the use of the robust design with transient capture–recapture models. *The Auk* 120:1151–1158.

Jankowski, J. E., G. A. Londoño, S. K. Robinson, and M. A. Chappell (2012). Exploring the role of physiology and biotic interactions in determining elevational ranges of tropical animals. *Ecography* 36:1–12.

Jarzyna, M. A., I. Quintero, and W. Jetz (2021). Global functional and phylogenetic structure of avian assemblages across elevation and latitude. *Ecology Letters* 24:196–207.

Johnson, E. I., and J. D. Wolfe (2016). *Molting in Neotropical Birds: Life History and Forest Fragmentation*. Taylor & Francis, CRC Press, Boca Raton, FL, USA.

Jones, S. E. I., J. A. Tobias, R. Freeman, and S. J. Portugal (2019). Weak asymmetric interspecific aggression and divergent habitat preferences at an elevational contact zone between tropical songbirds. *Ibis* 162:814–826.

Kaschube, D. R., J. F. Saracco, C. Ray, C. M. Godwin, K. R. Foster, and P. Pyle (2022). Minimum capture–recapture rates and years of banding station operations to obtain reliable adult annual survival estimates. *Journal of Field Ornithology* 93:7.

Kéry, M., and M. Schaub (2011). *Bayesian Population Analysis using WinBUGS: A Hierarchical Perspective*. Academic Press, New York, NY, USA.

Kittelberger, K. D., M. H. C. Neate-Clegg, E. R. Buechley, and Ç. H. Şekercioğlu (2021). Community characteristics of forest understory birds along an elevational gradient in the Horn of Africa: A multi-year baseline. *Ornithological Applications* 123:duad009.

Laake, J., and E. Rexstad (2006). RMark - an alternative approach to building linear models in MARK. In *Program MARK: A Gentle Introduction* (E. G. Cooch and G. C. White, Editors). Colorado State University, Fort Collins, CO, USA. pp. 1–111.

Lebreton, J.-D., K. P. Burnham, and D. R. Anderson (1992). Modeling survival and testing biological hypotheses using marked animals: A unified approach with case studies. *Ecological Monographs* 62:67–118.

Lenoir, J., R. Bertrand, L. Comte, L. Bourgeaud, T. Hattab, J. Murienne, and G. Grenouillet (2020). Species better track climate warming in the oceans than on land. *Nature Ecology and Evolution* 4:1044–1059.

Londoño, G. A., M. A. Chappell, J. E. Jankowski, and S. K. Robinson (2017). Do thermoregulatory costs limit altitude distributions of Andean forest birds? *Functional Ecology* 31:204–215.

Londoño, G. A., J. P. Gomez, M. A. Sánchez-Martínez, D. J. Levey, and S. K. Robinson (2023). Changing patterns of nest predation and predator communities along a tropical elevation gradient. *Ecology Letters* 26:609–620.

Maicher, V., S. Sáfián, M. Murkwe, S. Delabye, Ł. Przybyłowicz, P. Potocký, I. N. Kobe, Š. Janeček, J. E. J. Mertens, E. B. Fokam, T. Pyrcz, et al. (2020). Seasonal shifts of biodiversity patterns and species' elevation ranges of butterflies and moths along a complete rainforest elevational gradient on Mount Cameroon. *Journal of Biogeography* 47:342–354.

Martin, T. E. (2004). Avian life-history evolution has an eminent past: Does it have a bright future? *The Auk* 121:289–301.

Martin, T. E., S. E. I. Jones, T. J. Creedy, H. M. J. Hoskins, N. P. McCann, S. P. Batke, D. L. Kelly, J. E. Kolby, R. Downing, S. M. S. Zelaya, S. E. W. Green, et al. (2021). A review of the ecological value of Cusuco National Park: An urgent call for conservation action in a highly threatened Mesoamerican cloud forest. *Journal of Mesoamerican Biology* 1:6–50.

McCain, C., T. Szewczyk, and K. Bracy Knight (2016). Population variability complicates the accurate detection of climate change responses. *Global Change Biology* 22:2081–2093.

Myers, N., R. A. Mittermeier, C. G. Mittermeier, G. A. B. da Fonseca, and J. Kent (2000). Biodiversity hotspots for conservation priorities. *Nature* 403:853–858.

Neate-Clegg, M. H. C., M. A. Etterson, M. W. Tingley, and W. D. Newmark (2023). The combined effects of temperature and fragment area on the demographic rates of an Afro-tropical bird community over 34 years. *Biological Conservation* 282:110051.

Neate-Clegg, M. H. C., S. E. I. Jones, O. Burdekin, M. Jocque, and Ç. H. Şekercioğlu (2018). Elevational changes in the avian community of a Mesoamerican cloud forest park. *Biotropica* 50:805–815.

Neate-Clegg, M. H. C., S. E. I. Jones, J. A. Tobias, W. D. Newmark, and Ç. H. Şekercioğlu (2021a). Ecological correlates of elevational range shifts in tropical birds. *Frontiers in Ecology and Evolution* 9:621749.

Neate-Clegg, M. H. C., T. G. O'Brien, F. Mulindahabi, and Ç. H. Şekercioğlu (2020). A disconnect between upslope shifts and climate change in an Afro-tropical bird community. *Conservation Science and Practice* 2:e291.

Neate-Clegg, M. H. C., T. R. Stanley, Ç. H. Şekercioğlu, and W. D. Newmark (2021b). Temperature-associated decreases in demographic rates of Afro-tropical bird species over 30 years. *Global Change Biology* 27:2254–2268.

Neate-Clegg, M. H. C., S. N. Stuart, D. Mtui, Ç. H. Şekercioğlu, and W. D. Newmark (2021c). Afro-tropical montane birds experience upslope shifts and range contractions along a fragmented elevational gradient in response to global warming. *PLoS One* 16:e0248712.

Neate-Clegg, M. H. C., and M. W. Tingley (2023). Building a mechanistic understanding of climate-driven elevational shifts in birds. *PLoS Climate* 2:e0000174.

Pollock, H. S., C. E. Tarwater, J. R. Karr, and J. D. Brawn (2024). Long-term monitoring reveals the long lifespans of Neotropical forest landbirds. *Ecology* 105:e4386.

Pradel, R. (1996). Utilization of capture–mark–recapture for the study of recruitment and population growth rate. *Biometrics* 52:703–709.

Pradel, R., J. E. Hines, J.-D. Lebreton, and J. D. Nichols (1997). Capture–recapture survival models taking account of transients. *Biometrics* 53:60–72.

Pyle, P., M. Gahbauer, E. I. Johnson, T. B. Ryder, and J. D. Wolfe (2022). Application of a global age-coding system ("WRP"), based on molts and plumages, for use in demographic and other studies of birds. *Ornithology* 139:ukab063.

Quintero, I., and W. Jetz (2018). Global elevational diversity and diversification of birds. *Nature* 555:246–250.

R Core Team (2023). *R: A Language and Environment for Statistical Computing*. R Foundation for Statistical Computing, Vienna, Austria. <https://www.R-project.org/>

Rahbek, C., M. K. Borregaard, R. K. Colwell, B. Dalsgaard, B. G. Holt, N. Morueta-Holme, D. Nogués-Bravo, R. J. Whittaker, and J. Fjeldså (2019). Humboldt's enigma: What causes global patterns of mountain biodiversity? *Science* 365:1108–1113.

Rangel-Salazar, J. L., K. Martin, P. Marshall, and R. W. Elner (2008). Population dynamics of the ruddy-capped nightingale thrush (*Catharus frantzii*) in Chiapas, Mexico: Influences of density, productivity and survival. *Journal of Tropical Ecology* 24:583–593.

Robinson, R. A., R. Julliard, and J. F. Saracco (2009). Constant effort: Studying avian population processes using standardised ringing. *Ringing and Migration* 24:199–204.

Rubenstein, M. A., S. R. Weiskopf, R. Bertrand, S. L. Carter, L. Comte, M. J. Eaton, C. G. Johnson, J. Lenoir, A. J. Lynch, B. W. Miller, T. L. Morelli, et al. (2023). Climate change and the global redistribution of biodiversity: Substantial variation in empirical support for expected range shifts. *Environmental Evidence* 12:7.

Ruiz-Gutiérrez, V., P. F. Doherty, E. Santana, S. Contreras Martínez, J. Schondube, H. V. Munguía, and E. Iñigo-Elias (2012). Survival of resident Neotropical birds: Considerations for sampling and analysis based on 20 years of bird-banding efforts in Mexico. *The Auk* 500:500–509.

Ryder, T. B., and T. S. Sillett (2016). Climate, demography and lek stability in an Amazonian bird. *Proceedings of the Royal Society B* 283:20152314.

Le Saout, S., M. Hoffman, Y. Shi, A. Hughes, C. Bernard, T. M. Brooks, B. Bertzky, S. H. M. Butchart, S. N. Stuart, T. Badman, and A. S. L. Rodrigues (2013). Protected areas and effective biodiversity conservation. *Science* 342:803–804.

Saracco, J. F., P. Pyle, D. R. Kaschube, M. Kohler, C. M. Godwin, and K. R. Foster (2022). Demographic declines over time and variable responses of breeding bird populations to human footprint in the Athabasca Oil Sands Region, Alberta, Canada. *Ornithological Applications* 124:duac037.

Saracco, J. F., J. A. Royle, D. F. DeSante, and B. Gardner (2010). Modeling spatial variation in avian survival and residency probabilities. *Ecology* 91:1885–1891.

Scholer, M. N., P. Arcese, M. L. Puterman, G. A. Londoño, and J. E. Jankowski (2019). Survival is negatively related to basal metabolic rate in tropical Andean birds. *Functional Ecology* 33:1436–1445.

Scholer, M. N., M. Strimas-Mackey, and J. E. Jankowski (2020). A meta-analysis of global avian survival across species and latitude. *Ecology Letters* 23:1537–1549.

Şekercioğlu, C. H., R. B. Primack, and J. Wormworth (2012). The effects of climate change on tropical birds. *Biological Conservation* 148:1–18.

Sheldon, K. S. (2019). Climate change in the tropics: Ecological and evolutionary responses at low latitudes. *Annual Review of Ecology, Evolution, and Systematics* 50:303–333.

Srinivasan, U., and D. S. Wilcove (2021). Interactive impacts of climate change and land-use change on the demography of montane birds. *Ecology* 102:e03223.

Taylor, J., and O. Komar (2010). The Ruddy-capped Nightingale-Thrush (*Catharus frantzii*) in El Salvador: Notes on the life history and ecology of two isolated populations. *Ornitología Neotropical* 21:225–239.

Telenský, T., D. Storch, P. Klvaňa, and J. Reif (2023). Extension of Pradel capture–recapture survival-recruitment model accounting for transients. *Methods in Ecology and Evolution* 2023:1–13.

Tenan, S., R. Pradel, G. Tavecchia, J. M. Igual, A. Sanz-Aguilar, M. Genovart, and D. Oro (2014). Hierarchical modelling of population growth rate from individual capture–recapture data. *Methods in Ecology and Evolution* 5:606–614.

Tingley, M. W., M. S. Koo, C. Moritz, A. C. Rush, and S. R. Beissinger (2012). The push and pull of climate change causes heterogeneous shifts in avian elevational ranges. *Global Change Biology* 18:3279–3290.

Valcu, M., J. Dale, M. Griesser, S. Nakagawa, and B. Kempenaers (2014). Global gradients of avian longevity support the classic evolutionary theory of ageing. *Ecography* 37:930–938.

de Valpine, P., D. Turek, C. J. Paciorek, C. Anderson-Bergman, D. T. Lang, and R. Bodik (2017). Programming with models: Writing statistical algorithms for general model structures with NIMBLE. *Journal of Computational and Graphical Statistics* 27:403–413.

White, E. R. (2019). Minimum time required to detect population trends: The need for long-term monitoring programs. *BioScience* 69:26–39.

Wiersma, P., A. Munoz-Garcia, A. Walker, and J. B. Williams (2007). Tropical birds have a slow pace of life. *Proceedings of the National Academy of Sciences USA* 104:9340–9345.

Williams, J. W., and S. T. Jackson (2007). Novel climates, no-analog communities, and ecological surprises. *Frontiers in Ecology and the Environment* 5:475–482.

Williams, S. E., and A. De la Fuente (2021). Long-term changes in populations of rainforest birds in the Australia Wet Tropics bioregion: A climate-driven biodiversity emergency. *PLoS One* 16:1–16.

Wolfe, J. D., C. J. Ralph, and P. Elizondo (2015). Changes in the apparent survival of a tropical bird in response to the El Niño Southern Oscillation in mature and young forest in Costa Rica. *Oecologia* 178:715–721.

Wolfe, J. D., T. B. Ryder, and P. Pyle (2010). Using molt cycles to categorize the age of tropical birds: An integrative new system. *Journal of Field Ornithology* 81:186–194.

Woodworth, B. K., D. R. Norris, B. A. Graham, Z. A. Kahn, and D. J. Mennill (2018). Hot temperatures during the dry season reduce survival of a resident tropical bird. *Proceedings of the Royal Society B: Biological Sciences* 285:20180176.